

Spray Deposition and Characterization of Zirconium-Oxide Thin Films

A. ORTIZ,^{1,3} J.C. ALONSO,¹ and E. HARO-PONIATOWSKI²

1.—Instituto de Investigaciones en Materiales, Coyoacán 04510, D.F., México. 2.—Departamento de Física, Universidad Autónoma Metropolitana Iztapalapa, Iztapalapa 09340, D.F., México. 3.—E-mail: aortiz@servidor.unam.mx

Zirconium oxide films were prepared by the pyrosol process using zirconium acetylacetonate as source material onto clear fused quartz and (100) silicon at substrate temperatures ranging from 300°C to 575°C. X-ray diffraction (XRD) measurements show that samples prepared at substrate temperatures lower than 425°C are amorphous. Films deposited at higher temperatures and short deposition times show a cubic crystalline structure. However, for long deposition times, the samples show monoclinic crystalline structure. A similar phase transformation is observed on samples deposited at short time if they are annealed at high temperature. The cubic and monoclinic phases of the corresponding samples were confirmed by infrared (IR) and Raman spectroscopy, respectively. The ZrO₂ films with cubic phase show an almost stoichiometric chemical composition and refractive index values of the order of 2.1 with an energy band gap of 5.47 eV. The current-density electric-field characteristics of metal-oxide semiconductor (MOS) structures show a small ledge from 2 MV/cm to 4.5 MV/cm, indicating current injection and charge trapping. For higher electric fields, the current is associated with oxygen ion diffusion through the zirconium oxide film. The dielectric breakdown is observed at 6 MV/cm, which is a value higher than those observed in the monoclinic and tetragonal phases.

Key words: Thin films, oxide, pyrosol process, insulator

INTRODUCTION

Because of its physical and chemical properties, there is growing interest in research on thin-film deposition of zirconium oxide. Among the physical properties, from an electrical point of view, there is interest in zirconium oxide films as a possible high dielectric-constant material for very large-scale integrated circuits where it could replace silicon dioxide, for instance, in gate stack and for storage capacitors in dynamic random-access memories.^{1,2} This material has a relatively high refractive index; therefore, it has promising applications in optical engineering, such as low-loss laser mirrors, laser gyroscopes in guidance systems, high laser-power operation, interference filters, etc.³ Zirconium oxide is a promising material for practical applications

because of its high strength, toughness, and corrosion resistance at high temperatures.⁴ Zirconium oxide is being applied as a solid-state electrolyte of solid-oxide fuel cells⁵ and as a catalyst.⁶

Depending on the interest in a particular physical property, zirconium oxide films have been prepared on different kinds of substrates, such as silicon single-crystal wafers, glass slices, fused quartz slices, etc. Thin films of this material have been prepared by different techniques, such as growth from an aqueous solution,⁷ reactive pulsed-laser ablation,⁸ sol-gel process,⁹ metal-organic chemical vapor deposition (MOCVD),¹⁰ electron beam evaporation,¹¹ chemical vapor deposition (CVD),¹² ion-beam-assisted evaporation,¹³ sputtering,¹⁴ and spray pyrolysis.¹⁵ Several zirconium-source materials have been used; some examples are metallic zirconium, zirconium chloride, mixtures of Zr n-propoxide and propanol, zirconium acetylacetonate, mixtures of Zr

(Received May 6, 2004; accepted June 7, 2004)

trifluoroacetylacetonate and oxygen gas, etc. Among the deposition techniques and zirconium-source materials, the ultrasonic spray pyrolysis method, also called pyrosol, has been well described in several reports.^{16,17} This method is considered as a CVD process when the deposition parameters are optimized. This feature permits deposit films with a root mean-square roughness as low as 1 nm. It does not require expensive vacuum equipment, and it is possible to prepare uniform high-quality thin films on relatively large areas by moving the substrate and/or the nozzle device. It is probably the easiest and lowest cost process to produce thin films. On the other hand, zirconium acetylacetonate is an organometallic compound that is inexpensive, nontoxic, and stable in air atmosphere at room temperature.

In this work, we report the structural, optical, and electrical properties of undoped, zirconium-oxide thin films deposited by the ultrasonic spray-pyrolysis method using zirconium acetylacetonate (ZAcAc) dissolved in pure methanol at air atmosphere.

EXPERIMENTAL

The zirconium oxide films were deposited by the pyrosol process. The start solution was 0.025-M zirconium acetylacetonate in pure methanol. There was no necessity to add acetic acid to get the complete dissolution of the source material; the solution was transparent. The substrate temperature (T_s) was varied from 300°C to 575°C in steps of 25°C. The carrier gas and director gas flow rate, air in both cases, were fixed at 3.5 L/min and 1.5 L/min, respectively. It is well known that, in general, the thickness of films deposited by spray pyrolysis decreases as the substrate temperature increases.¹⁸ Therefore, in order to obtain films with similar thickness, the deposition time (t_d) was varied from 5 min to 10 min. The substrates used in this work were pyrex glass slices; clear fused quartz slices, ultrasonically cleaned with trichloroethylene, acetone, and methanol; and (100) n-type silicon single-crystal slices with 200 Ω cm electrical resistivity, chemically cleaned with a P etch solution [H_2O (300 mL), HF (15 mL), HNO_3 (10 mL)] in order to remove the native oxide from the surface of the silicon slices.¹⁹ The films deposited onto pyrex glass were used to measure the thickness; in these cases, a small part of the substrate was covered with a cover pyrex glass to form a step during deposition. The thickness (t_h) of the deposited films was measured with a Sloan Dektac IIA profilometer. In order to perform Raman spectroscopic measurements, a set of thicker samples was prepared at $T_s = 550^\circ\text{C}$ with a deposition time of 70 min using clear fused quartz as substrates. These samples were annealed at 900°C in air for 2 h. X-ray diffraction (XRD) spectra were obtained with a Siemens D-500 diffractometer (Munich, Germany) using a $\text{CuK}\alpha_1$ wavelength (1.54056 Å). The films deposited onto c-Si slices were used to measure the refractive index and thickness by ellipsometry with a Gaertner 117A ellipsometer

(Skokie, IL) using the 632-nm line from a He-Ne laser. Infrared (IR) transmittance measurements were carried out on these samples with a Fourier transform IR (FTIR) 205 Nicolet spectrophotometer. Raman spectroscopic measurements were performed at room temperature in air with a Spex 1403 double monochromator using the 514.5-nm line of an argon laser (Lexel, Farmingdale, NY) at a power level of 200 mW. The signal was detected with a photomultiplier and a standard photon-counting system. Optical transmission measurements in the wavelength range from 190 nm to 110 nm were performed with a double-beam Shimadzu UV-Vis 260 spectrophotometer (Kyoto, Japan) for the samples deposited onto clear fused quartz, with air in the reference beam. In order to evaluate the electrical characteristics of the zirconium oxide, some films were deposited onto (100) n-type silicon single-crystalline wafers with 2- Ω cm resistivity. The wafers were cleaned by the standard RCA process prior to deposition. Electrical contact to the films was provided by aluminum dots deposited by vacuum thermal evaporation through a metallic mask. The 1.12-mm diameter dots formed metal-oxide semiconductor (MOS) structures. The c-Si wafer was contacted by means of an eutectic In-Ga alloy; the wafer was placed on a gold-coated pedestal. The electrical contact on the aluminum dots was made with a gold-coated tungsten needle supported by a micromanipulator to assure ohmic contact. Current-voltage data were obtained with a computer interfaced arrangement incorporating a Keithley 485 picoammeter and a Keithley 230 programmable voltage source (Cleveland, OH).

RESULTS AND DISCUSSION

The XRD spectra for samples deposited at substrate temperatures from 300°C to 425°C correspond to materials of amorphous nature because there are no peaks associated with a crystalline phase. The amorphous nature of materials deposited at low T_s is explained considering that, at those low substrate temperatures, the impinging material does not have high enough surface mobility to produce the growing of a crystalline phase. However, the XRD spectra for samples with T_s higher than 425°C show a small and very broad peak located at approximately $2\theta = 30^\circ$. The intensity of this peak and other peaks located at about 37° and 50° increases as the substrate temperature increases. Figure 1 shows the XRD spectra for samples prepared at 525°C and 575°C. All the spectra show a crystalline phase that corresponds to a cubic crystalline structure. For higher substrate temperatures, the adatoms have high enough surface mobility to generate a crystalline material. However, the crystalline phase produced is the cubic phase, which, in principle, is not stable at low temperatures. This cubic phase becomes easily stabilized by alloying zirconium oxide with other oxides.²⁰ This apparently indicates that the deposited material is alloyed with another oxide; however, no peaks

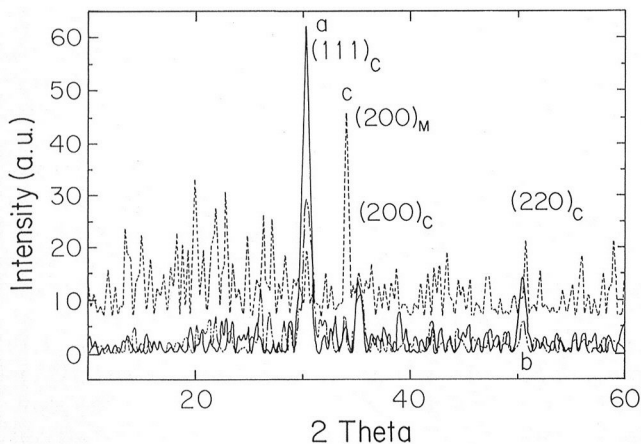


Fig. 1. The XRD spectra for ZrO_2 thin films prepared at substrate temperature of (a) 525°C and (b) 575°C. The spectrum c was obtained for a sample deposited at 575°C with a long deposition time.

pertaining to other materials are detected in the XRD spectra, and the diffraction peaks are well identified with the cubic phase. On the other hand, the XRD spectrum for a zirconium oxide film prepared at $T_s = 575^\circ\text{C}$ for deposition times of at least 35 min, keeping constant all others deposition parameters, shows a diffraction peak located at 34.16° , which can be associated with reflections on the (200) family planes of the monoclinic phase (baddeleyite), as is shown in Fig. 1c. It is well known that the monoclinic phase is the one stable phase at low temperatures, and that the cubic phase is stable at temperatures from 2,370°C to the melting point at 2,680°C.²¹ The observed phase transformation in the sample prepared with the longest deposition time indicates that alloying of ZrO_2 is not a suitable explanation for the cubic phase. It appears that initially deposited layers crystallize in a cubic phase, which is unstable, for short deposition times, as a transition step toward the crystallization in the monoclinic phase. It has been reported that the x-ray spectra of nanosized zirconium (hydrous) oxide particles subjected to ultrasonic energy and calcinated at 500°C show a cubic crystalline phase.²² In that case, the cubic phase is obtained as a result of the sonication process, the ultrasonic energy produce structural transformation in the zirconium (hydrous) oxide stabilizing the cubic phase at room temperature. However, the cubic phase in those particles recrystallizes into the tetragonal phase, for calcinations at temperatures higher than 550°C during 7 h. In the present work, ultrasonic energy is used to generate the small drops of the start solution for the spray deposition, but when zirconium oxide is synthesized, it is not sonicated. At present, it is not clear how the cubic phase is formed, although relatively long thermal processes induce a structural transformation. More work is necessary to get a complete explanation of the observed behavior.

The films thickness values, measured for several points on the deposited surface with both the profilometer and the ellipsometer, do not show great

differences among them, indicating good film uniformity on the surface area of the substrates (1 cm \times 1 cm). The thickness of films deposited at lowest substrate temperature is of the order of 200 nm; while the thickness for crystalline films ($T_s > 425^\circ\text{C}$) has values in the range from 100 nm to 150 nm. Taking into account these thickness values, the deposition rate was determined as a function of the substrate temperature. Figure 2 shows that the deposition rate decreases as the substrate temperature increases. This is a common behavior observed in films prepared by the spray pyrolysis process¹⁸ because the amount of precursors related with zirconium impinging on the substrate decreases as its temperature increases because of evaporation of the solvent in the small drops and the zirconium-source material.

The refractive index values obtained from the ellipsometry measurements are shown in Fig. 3, as a function of the substrate temperature. The refractive index increases as T_s increases; however, the increment rate in the range from 300°C to 425°C is slow. Because all these samples correspond to deposited materials of amorphous nature, the observed increment is explained considering that, as T_s increases, the organic radicals related with the

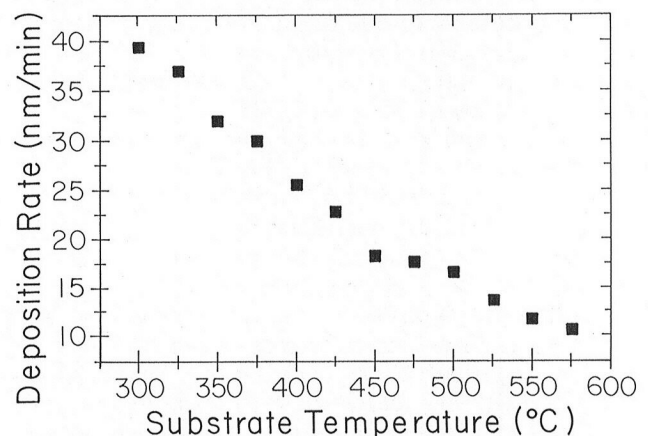


Fig. 2. Dependence of the deposition rate as a function of the substrate temperature. The decreasing behavior is a common trend observed in spray-pyrolysis-deposited films.

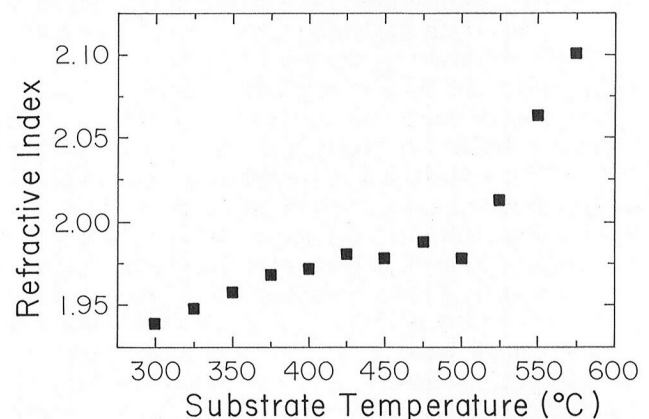


Fig. 3. Variation of the refractive index of ZrO_2 films as a function of the substrate temperature.

zirconium-source material are evaporated in a more efficient way, resulting in a denser zirconium-oxide film. The refractive index is almost constant for Ts in the range from 425°C to 500°C. In this range, the deposited material starts having a cubic crystalline structure, as is shown by the XRD spectra. The refractive index increases substantially as the substrate temperature is increased from 525°C to 575°C. This change in the refractive index is associated with a densification process and grain growth in the polycrystalline-deposited material, as is shown by the XRD results. It should be remarked that the value of 2.1 for the refractive index is similar to those reported for bulk samples with monoclinic crystalline structure.²³ This fact indicates that a dense and an almost stoichiometric material is produced at those substrate temperatures.

The results of relative chemical composition determined from wavelength-dispersive spectroscopy measurements for some selected samples are shown in Table I. For the sample deposited at 325°C, formed by an amorphous material, the ratio of oxygen/zirconium shows that the deposited material is a zirconium-rich material in comparison with the stoichiometric chemical composition. This fact can be explained considering that, at those low Ts, the chemical reaction forming the zirconium oxide is not complete, and the zirconium is not fully oxidized. The samples deposited at higher substrate temperatures have relative chemical compositions that almost correspond to that of stoichiometric materials with values of the O/Zr ratio near 2. At these Ts, the deposited materials show the cubic crystalline phase, in which the zirconium is completely oxidized. It should be remarked that no signal related to carbon presence was observed.

Figure 4 shows the optical transmission spectra for samples prepared at substrate temperatures of 550°C (Fig. 4a) and 575°C (Fig. 4b). It can be observed that the average optical transmission is about 80% for both samples. From these spectra, using the method developed by Swanepoel,²⁴ the refractive index and the absorption coefficient were determined. The refractive index is almost constant for all the studied photon wavelengths range with a value of 2.05. This value is in agreement with the one calculated from ellipsometric measurements. On the other hand, this value is higher than those determined for the monoclinic phase (1.84) and for

Table I. Thickness and Chemical Composition Obtained by Wavelength Dispersive Spectroscopy of Zirconium Oxide Films Prepared by the Pyrosol Process

T _s (°C)	th (nm)	Zr (at.%)	O (at.%)
325	175	37.6	62.4
425	157	31.9	68.1
525	100	31.6	68.4

Note: th = thickness of films.

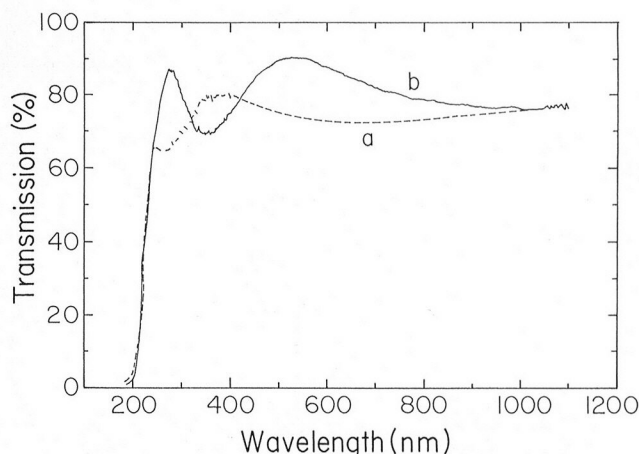


Fig. 4. Optical transmission spectra for ZrO₂ films deposited at (a) 525°C and (b) 575°C. The absorption edge corresponds to an energy band gap of 5.47 eV.

the tetragonal phase (1.93) in thin films deposited by reactive electron-beam evaporation at room temperature and 260°C, respectively.²⁵ The value associated with the monoclinic phase is much lower than that reported for bulk samples. The observed difference can be due to the density of the film prepared at relatively low substrate temperature. It is well known that the refractive index values depend on the crystalline phase of the zirconium oxide. In the present work, the obtained refractive index could be associated with the cubic phase; however, to the best of our knowledge, the refractive index for the cubic phase has not been reported. Considering that zirconium oxide has direct interband electronic transitions, a value of 5.47 eV for its energy band gap was measured. This value is lower than that reported for ZrO₂ films prepared by spray pyrolysis (5.68 eV) with monoclinic crystalline phase.¹⁵ However, the energy band gap measured in the present work is higher than those values reported for films with monoclinic phase (5.12 eV) deposited by the CVD process at substrate temperatures in the range from 800°C to 1,000°C.²⁶ Given the wide dispersion in the refractive index and energy band gap values, even for single crystalline samples, it is difficult to compare the present results with previous ones.

Figure 5 shows the IR spectrum for a sample deposited at 550°C. There are absorption peaks located at 460 cm⁻¹, 1,070 cm⁻¹, 1,630 cm⁻¹, and 3,880 cm⁻¹. The peak at 1,070 cm⁻¹ is associated with the stretching mode vibration of silicon dioxide.²⁷ This silicon dioxide is formed during film deposition at the interface between the zirconium oxide film and the crystalline silicon substrate. The peak at 460 cm⁻¹ is associated with the Zr-O vibration in a cubic crystalline structure.²² This result is in agreement with those obtained from XRD. There is a clear difference with the localization of IR absorption peaks in the tetragonal phase (350 cm⁻¹, 485 cm⁻¹, and 590 cm⁻¹) and in the monoclinic phase (404 cm⁻¹, 490 cm⁻¹, and 575 cm⁻¹).²⁶ The absorption bands located at 1,630 cm⁻¹ and 3,380 cm⁻¹ are associated with the

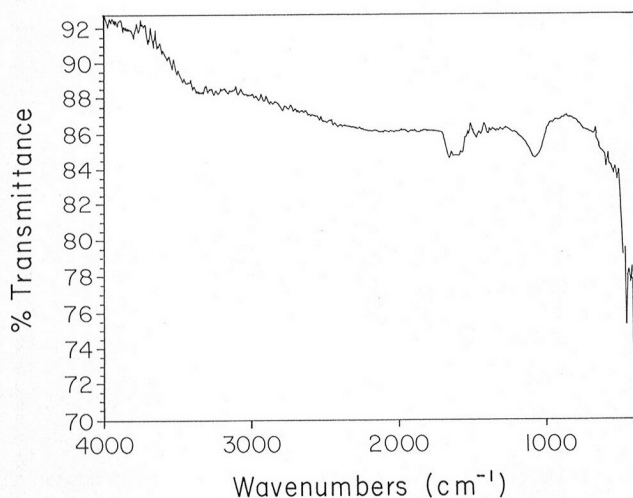


Fig. 5. Typical IR transmission spectrum of a spray-pyrolysis ZrO_2 thin film prepared at a substrate temperature higher than $525^\circ C$.

presence of O-H groups. Probably the deposited films absorb water from the atmosphere after deposition.

The XRD spectra (not shown) of samples prepared for Raman spectroscopy measurements, annealed in air at $900^\circ C$ for 2 h, show peaks that are associated with the monoclinic phase. Figure 6 shows the corresponding Raman spectrum. This spectrum shows well-defined peaks located at 176.4 cm^{-1} , 189.0 cm^{-1} , 219.4 cm^{-1} , 305.0 cm^{-1} , 332.0 cm^{-1} , 345.0 cm^{-1} , 379.8 cm^{-1} , 474.7 cm^{-1} , 535.4 cm^{-1} , 560.0 cm^{-1} , 615.6 cm^{-1} , and 639.0 cm^{-1} that are attributed to monoclinic phase, and only one peak, located at 264.3 cm^{-1} , associated with the tetragonal phase.^{28,29} It should be remarked that the position of these peaks are slightly different in comparison with those obtained for fully monoclinic powder. These small differences can be associated with the slight deviation of chemical composition from that stoichiometric composition and with the existence of internal stresses in the present case.

Figure 7 shows the electrical characteristics of a metal/insulator/semiconductor structure with a zirconium oxide film deposited at $550^\circ C$ with a thick-

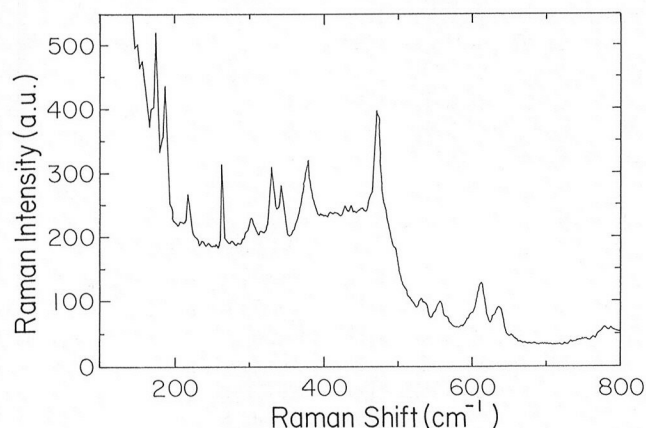


Fig. 6. Raman spectrum for an annealed ZrO_2 film. Most of the observed peaks are associated with the monoclinic phase of ZrO_2 .

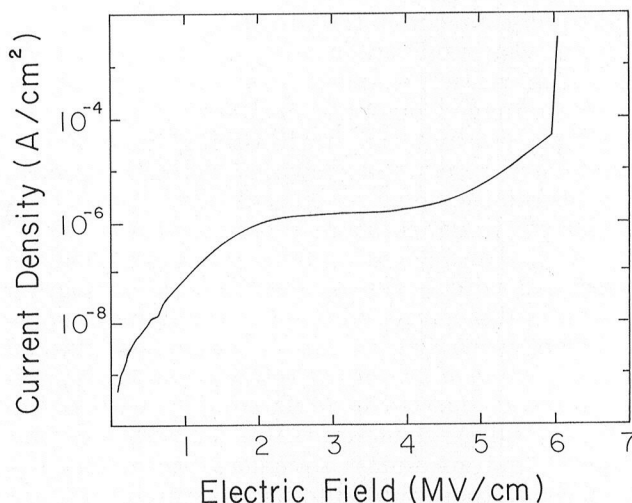


Fig. 7. Current-density-applied electric field for a MOS structure where a ZrO_2 film was incorporated as the insulator film.

ness of 113 nm onto a (100) p-type silicon wafer with electrical resistivity of $2\ \Omega\text{cm}$. In this figure, it can be observed that the current density measured for electric fields below 1 MV/cm is of the order of 10^{-8} A/cm^2 . It is associated with the displacement current because of the ramped applied voltage. For applied electric fields between 1 MV/cm and 2 MV/cm, the current density increases up to values of the order of 10^{-6} A/cm^2 . This behavior is related to current injection across the insulating film. For electric fields higher than 2 MV/cm, the current density increases slowly up to electric breakdown at electric fields of the order of 6 MV/cm. In this range, the current density is higher than $1\ \mu\text{A/cm}^2$. This current could be associated with oxygen ion diffusion through the zirconium oxide film because it is well known that ZrO_2 is an ionic conductor at temperatures under $1,000^\circ C$. A similar behavior has been observed in ZrO_2 films deposited onto silicon substrates by MOCVD. However, the electrical resistivity, in this region, is of the order of $10^{12}\ \Omega\text{cm}$. This relatively high electrical resistivity value can be explained, in part, by the existence of interfacial silicon oxide generated during deposition, as is observed, in IR spectroscopy, although normally the quality of these silicon oxide films is too low. The relatively high, breakdown electric field could be related to the cubic phase of the deposited material. In general, for monoclinic and tetragonal phases, the breakdown electric fields measured are of the order of 1–2 MV/cm.^{10,23}

CONCLUSIONS

Cubic-phase zirconium-oxide films were deposited by ultrasonic spray-pyrolysis process at substrate temperatures higher than $425^\circ C$. This cubic phase is confirmed by an IR absorption band located at 460 cm^{-1} . These films show an almost stoichiometric chemical composition ($O/Zr \approx 2$), refractive index values around 2.1, and an optical energy band gap of 5.47 eV. Breakdown electric fields of the order of

6 MV/cm were observed for these films. However, there is a phase transformation toward the monoclinic phase by both (a) using longer deposition times during film growth and (b) annealing the films at 900°C for 2 h.

ACKNOWLEDGEMENTS

The authors thank M.A. Canseco, S. Jimenez, J. Camacho, and M.A. Camacho for technical assistance. This work was supported by DGAPA-UNAM under Contract No. IN10997.

REFERENCES

1. J. Shappir, A. Anis, and I. Pinsky, *IEEE Trans. Elec. Dev.* Ed-33, 442 (1986).
2. D.K. Fork, D.B. Fenner, G.A.N. Connell, J.M. Phillips, and T.H. Geballe, *Appl. Phys. Lett.* 57, 1137 (1990).
3. X. Aslanoglou, P.A. Assimakopoulos, G. Trapalis, G. Kordas, M.A. Karukassides, and M. Pilakouta, *Nucl. Instrum. Meth. Phys. Res.* B118, 630 (1996).
4. H. Hasuyama, Y. Shima, K. Baba, G.K. Wolf, H. Martín, and F. Stippich, *Nucl. Instrum. Meth. Phys. Res.* B127/128, 827 (1997).
5. O. Yamamoto, Y. Arati, Y. Takeda, N. Imanishi, Y. Mizutani, M. Kawai, and Y. Nakamura, *Solid State Ionics* 79, 137 (1995).
6. T.M. Miller and V.H. Grassian, *J. Am. Chem. Soc.* 117, 10969 (1995).
7. T. Yao, T. Inui, and A. Ariyoshi, *J. Am. Ceram. Soc.* 79, 3329 (1996).
8. C. Flamini, A. Giardini Guidoni, R. Teghil, and V. Marotta, *Appl. Surf. Sci.* 138/139, 344 (1999).
9. R. Brenier, C. Urlacher, J. Mugnier, and M. Brunel, *Thin Solid Films* 338, 136 (1999).
10. C.S. Hwang and H.J. Kim, *J. Mater. Res.* 8, 1361 (1993).
11. K.H. Muller, R.P. Netterfield, and P.J. Martin, *Phys. Rev. B* 35, 2934 (1987).
12. J.S. Kim, H.A. Marzouk, and P.J. Rencroff, *Thin Solid Films* 254, 33 (1995).
13. M. Matsuoka, S. Isotani, S. Miyake, S. Setsuhara, K. Ogata, and N. Kuratani, *J. Appl. Phys.* 80, 1177 (1996).
14. Y.M. Sun, J. Lozano, H. Ho, H.J. Park, S. Veldaman, and J.M. White, *Appl. Surf. Sci.* 16, 115 (2000).
15. Y.M. Gao, P. Wu, R. Kershaw, K. Dwight, and A. Wols, *Mater. Res. Bull.* 25, 871 (1990).
16. M. Langlet and J.C. Jaubert, in *Chemistry of Advanced Materials, Pyrosol Process or the Pyrolysis of an Ultrasonically Generated Aerosol*, ed. C.N.R. Rao (Oxford: Blackwell Scientific, 1993), p. 55.
17. J.C. Viguie and J. Spitz, *J. Electrochem. Soc.* 122, 565 (1975).
18. J. Aranovich, A. Ortiz, and R.H. Bube, *J. Vac. Sci. Technol.* 16, 994 (1979).
19. W.A. Pliskin and R.P. Gnall, *J. Electrochem. Soc.* 111, 872 (1964).
20. M. Matsuoka, S. Isotani, J.F.D. Chubaci, S. Miyake, Y. Setsuhara, K. Ogata, and N. Kuratani, *J. Appl. Phys.* 88, 3773 (2000).
21. H.Y. Zhu, T. Hirata, and Y. Maramatsu, *J. Am. Ceram. Soc.* 50, 2843 (1992).
22. L.A. Perez-Maqueda and E. Matijevic, *J. Mater. Res.* 12, 3286 (1997).
23. T.S. Kalkur and Y.C. Lu, *Thin Solid Films* 207, 193 (1992).
24. R. Swanepoel, *J. Phys. E: Sci. Instrum.* 16, 1214 (1983).
25. D. Reicher and K. Jungling, *Appl. Opt.* 36, 1626 (1997).
26. R.N. Tauber, A.C. Dunbri, and R.E. Caffrey, *J. Electrochem. Soc.* 118, 747 (1971).
27. P.G. Pai, S.S. Chao, Y. Takagi, and G. Lucovsky, *J. Vac. Sci. Technol.* A4, 698 (1986).
28. P. Barberis, T. Merle-Mejean, and P. Quintard, *J. Nucl. Mater.* 246, 232 (1997).
29. M. Jouanne, J.F. Morhange, M. Kanehisa, E. Haro-Poniatowski, G.A. Fuentes, E. Torres, and E. Hernández Téllez, *Phys. Rev. B* 64, 155404 (2001).